

Structural Characterization of the N-terminal Oligomerization Domain of the Bacterial Chromatin-structuring Protein, H-NS

Debora Renzoni¹, Diego Esposito¹, Mark Pfuhl¹, Jay C. D. Hinton²
Christopher F. Higgins³, Paul C. Driscoll^{1,4} and John E. Ladbury^{1*}

¹Department of Biochemistry & Molecular Biology, University College London, Gower Street London WC1E 6BT, UK

²Institute of Food Research Norwich Research Park Colney Norwich NR4 7UA, UK

³MRC Clinical Sciences Centre Imperial College School of Medicine, Hammersmith Hospital Campus, DuCane Road, London W12 0NN, UK

⁴The Ludwig Institute for Cancer Research, 91 Riding House Street, London W1P 8BT, UK

The H-NS protein plays a key role in condensing DNA and modulating gene expression in bacterial nucleoids. The mechanism by which this is achieved is dependent, at least in part, on the oligomerization of the protein. H-NS consists of two distinct domains; the N-terminal domain responsible for protein oligomerization, and the C-terminal DNA binding domain, which are separated by a flexible linker region. We present a multidimensional NMR study of the amino-terminal 64 residues of H-NS (denoted H-NS₁₋₆₄) from *Salmonella typhimurium*, which constitute the oligomerization domain. This domain exists as a homotrimer, which is predicted to be self-associated through a coiled-coil configuration. NMR spectra show an equivalent magnetic environment for each monomer indicating that the polypeptide chains are arranged in parallel with complete 3-fold symmetry. Despite the limited resonance dispersion, an almost complete backbone assignment for ¹H^N, ¹H^α, ¹⁵N, ¹³CO and ¹³C^α NMR resonances was obtained using a suite of triple resonance experiments applied to uniformly ¹⁵N-, ¹³C/¹⁵N- and ²H/¹³C/¹⁵N-labelled H-NS₁₋₆₄ samples. The secondary structure of H-NS₁₋₆₄ has been identified on the basis of the analysis of ¹H^α, ¹³C^α, ¹³C^β and ¹³CO chemical shifts, NH/solvent exchange rates, intra-chain H^N-H^N and medium-range nuclear Overhauser enhancements (NOEs). Within the context of the homotrimer, each H-NS₁₋₆₄ protomer consists of three α-helices spanning residues 2-8, 12-20 and 22-53, respectively. A topological model is presented for the symmetric H-NS₁₋₆₄ trimer based upon the combined analysis of the helical elements and the pattern of backbone amide group ¹⁵N nuclear relaxation rates within the context of axially asymmetric diffusion tensor. In this model, the longest of the three helices (helix 3, residues 22-53) forms a coiled-coil interface with the other chains in the homotrimer. The two shorter N-terminal helices fold back onto the outer surface of the coiled-coil core and potentially act to stabilise this configuration.

© 2001 Academic Press

Keywords: nuclear magnetic resonance; secondary structure; coiled-coil; H-NS; oligomerization

*Corresponding author

Abbreviations used: The one-letter code for amino acids is used. H-NS, wild-type H-NS from *Salmonella typhimurium*; H-NS_{C20S}, H-NS with the cysteine at position 20 replaced by serine and including an N-terminal GSHM-sequence derived from the cloning vector; H-NS₁₋₆₄, the N-terminal 68 residues of H-NS_{C20S} as described above including the GSHM-tag and the first 64 residues of the H-NS sequence; KP_i, potassium phosphate buffer; NOE, nuclear Overhauser effect; NOESY, NOE spectroscopy; HSQC, heteronuclear single quantum correlation.

E-mail address of the corresponding author: j.ladbury@biochem.ucl.ac.uk

Introduction

H-NS is involved in the condensation of bacterial DNA and controls the expression of about 30 known genes, mainly as a negative regulator of transcription (Spassky *et al.*, 1984; Drlica & Rouviere-Yaniv, 1987; Bertin *et al.*, 1990; Higgins *et al.*, 1990; Ussery *et al.*, 1994; Laurent-Winter *et al.*, 1997). The packaging of bacterial chromosomal DNA is thought to be *via* oligomerisation of a small group of proteins, of which H-NS is an important member. These provide a protein

scaffold with which DNA is associated. The H-NS protein is composed of 136 amino acid residues, and comprises at least two functional domains: a C-terminal domain involved in DNA binding and an N-terminal domain responsible for protein-protein interactions and homo-oligomerisation (Ueguchi *et al.*, 1997; Smyth *et al.*, 2000). The N and C-terminal domains are separated by a flexible linker region (Smyth *et al.*, 2000). The oligomerisation of H-NS is fundamental to its function, since a truncated form of the protein (containing only 63 or 64 residues from the N terminus) that is able to form heterodimers/oligomers with full-length H-NS protein *in vitro*, exhibits a dominant negative effect on the regulation of gene transcription by intact H-NS (Williams *et al.*, 1996; Ueguchi, *et al.*, 1996, 1997).

Previously we demonstrated that full-length H-NS from *Salmonella typhimurium* is capable of forming large, heterodisperse homo-oligomers, of a size which is dependent upon the concentration of the protein. A truncated form of the H-NS protein (residues 1-89), which lacks only the C-terminal DNA-binding domain, is able to adopt a range of oligomeric states similar to that of the full-length protein. However, a polypeptide comprising the N-terminal 64 residues of H-NS (H-NS₁₋₆₄) self-associates to form a hydrodynamically discrete homotrimeric species. Amino acid sequence analysis and secondary structure predictions suggest that this homotrimer is likely to be dominated by contributions from an α -helical coiled-coil conformation. We hypothesised that this trimeric unit represents a building block for the higher-order structure which forms the basis of the full-length H-NS-mediated scaffold for DNA packaging (Smyth *et al.*, 2000).

Although the three-dimensional solution structure has previously been described for the C-terminal DNA-binding domain of H-NS (residues 89-136, Shindo *et al.*, 1995, 1999), to date no high-resolution structural analysis of the N-terminal domain has been reported. We have found that HNS₁₋₆₄ yields NMR spectra that, although exhibiting very poor chemical shift dispersion, are amenable to investigation by multi-dimensional heteronuclear NMR methods. Here we report the polypeptide backbone resonance assignments and predicted secondary structural features of the N-terminal domain of H-NS₁₋₆₄ determined by ¹⁵N, ¹³C and ²H-isotope labelling and heteronuclear NMR spectroscopy. In addition we present a model for the global fold of the N-terminal domain of H-NS based upon the combined analysis of the regular secondary structure elements and the pattern of backbone amide bond ¹⁵N nuclear relaxation rates analysed within the framework of an axially asymmetric diffusion tensor.

Results and Discussion

Determination of the secondary structure of residues 1-64 of H-NS

NMR spectra for full-length H-NS showed that narrow lines were only obtained for residues corresponding to the C-terminal DNA-binding domain. The resonances of the N-terminal oligomerisation domain were obscured by extreme line broadening, thereby precluding structural analysis of the full length protein. To enable structural determination of the N terminus of the protein a series of truncated H-NS constructs were made. In this work we focussed on the analysis of the heteronuclear NMR spectra for the H-NS₁₋₆₄ polypeptide construct which is known to form a hydrodynamically discrete homotrimer species (Smyth *et al.*, 2000).

We expressed and labelled *S. typhimurium* H-NS₁₋₆₄ with stable NMR-active isotopes allowing the use of triple resonance heteronuclear NMR experiments. The cysteine at position 20 in the wild-type protein, which is not highly conserved among the known sequences of bacterial H-NS homologues, was replaced by serine to prevent inter-subunit disulphide bond formation (Smyth *et al.*, 2000). We showed previously that this mutation has no effect on the protein structure and function, since wild-type H-NS and H-NS_{C20S} show the same CD spectrum and thermal melting characteristics, and possesses a similar binding affinity for DNA.

Figure 1 displays the 2D ¹⁵N-¹H HSQC spectrum for a uniformly labelled sample of HNS₁₋₆₄. This spectrum, although yielding relatively poor chemical shift dispersion, shows only a single cross-peak for each residue in the polypeptide, consistent with a symmetric homo-oligomeric structure. The initial NMR experiments for resonance assignment were performed with a uniformly ²H/¹⁵N/¹³C-labelled H-NS₁₋₆₄ sample. An enhancement in the sensitivity and resolution of the spectra from a reduction of the detrimental nuclear relaxation effects that arise for large molecules in solution was obtained by perdeuteration of the sample (LeMaster & Richards, 1988; Torchia *et al.*, 1988). A set of triple resonance experiments that provided 3D HNCA, HN(CO)CA, HN(COCA)CB, HN(CA)CB, HNCO, HN(CA)CO datasets were used to obtain sequence-specific assignments of the NMR signals of the polypeptide backbone. 3D ¹⁵N NOESY-HSQC and ¹⁵N TOCSY-HSQC spectra recorded on a uniformly ¹⁵N-labelled sample were used to assign ¹H α signals. Using these experiments an almost complete backbone ¹H^N, ¹H α , ¹⁵N, ¹³C and ¹³CO assignment was possible (the chemical shift assignments have been submitted to the BioMagResBank; BMRB 4802). The triple resonance NMR experiments were also performed on a ¹⁵N/¹³C-labelled sample in order to account for the deuterium isotope effect on chemical shift values. A partial assignment of the ¹H and ¹³C side-chain

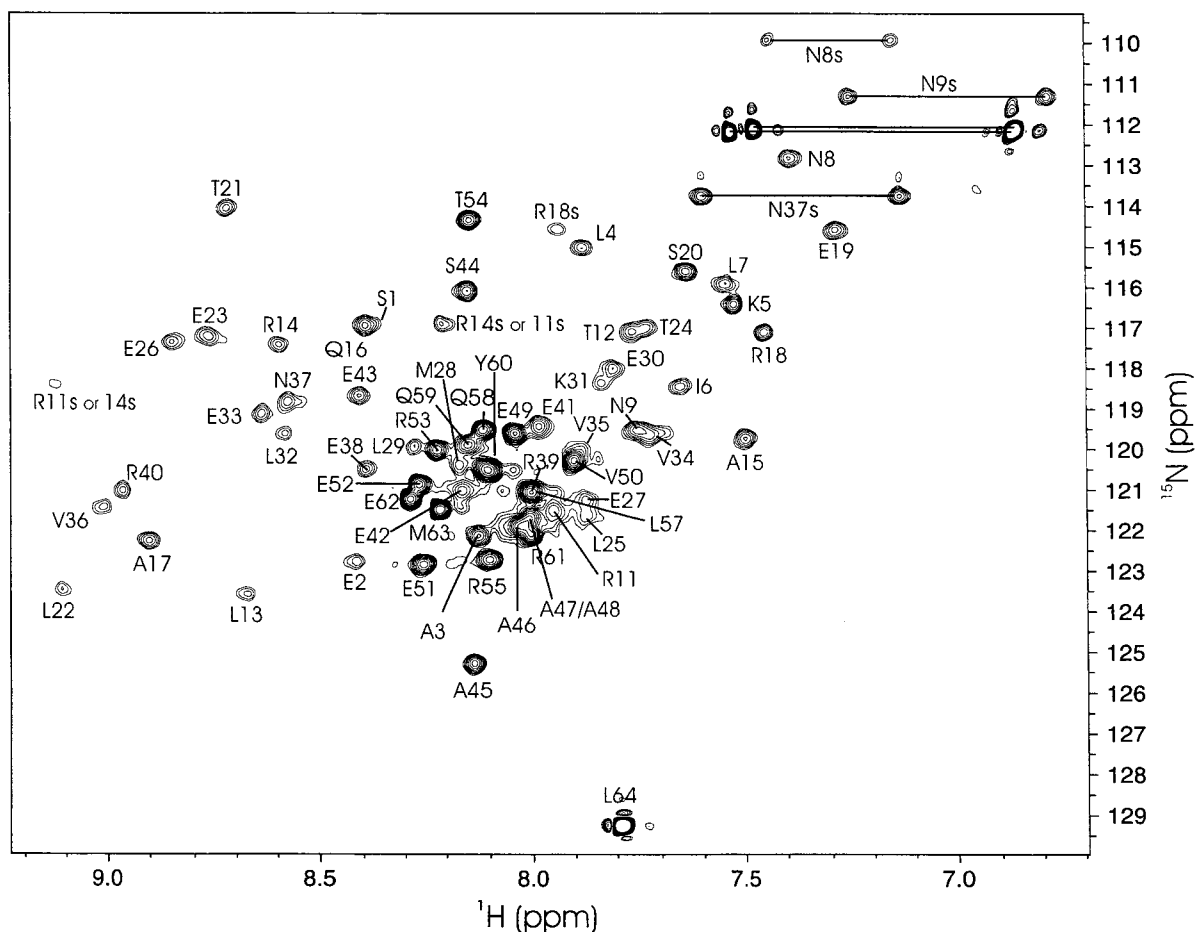


Figure 1. 2D ^1H - ^{15}N HSQC spectrum of H-NS $_{1-64}$ recorded at 600 MHz and 25°C. The buffer is 20 mM KP $_i$, 300 mM NaCl and 1 mM EDTA at pH 7.0, 10% $^2\text{H}_2\text{O}$. The monomer concentration was 1.5 mM. Residue-specific cross-peak assignments are indicated; s denotes a side-chain NH group.

resonances has been obtained from the analysis of a three-dimensional ^{13}C - ^{13}C nuclear Overhauser effect (NOE) experiment recorded at 800 MHz (Fischer *et al.*, 1996). The assignment of the backbone and the side-chain signals proved extremely difficult due to the substantial resonance overlap in the spectrum. This signal overlap is due both to the dominant contribution of α -helical secondary structure and the primary sequence of the HNS $_{1-64}$ polypeptide which contains few aromatic residues, several identical amino acid motifs, and strings of consecutive identical amino acids (see H-NS $_{1-64}$ primary sequence in Figure 2).

We analysed the NOESY spectra of HNS $_{1-64}$ to obtain short and medium-range interproton NOE contacts to assist the characterisation of the secondary structure. The majority of $\text{H}^{\text{N}}(i)$ - $\text{H}^{\text{N}}(i+1)$ and $\text{H}^{\text{N}}(i)$ - $\text{H}^{\text{N}}(i+3)$ NOEs were obtained from a ^{15}N -separated NOESY-HSQC spectrum recorded with an 80 ms NOE mixing time. A 3D version of the 4D ^{15}N , ^{15}N HSQC-NOESY-HSQC experiment (Kay *et al.*, 1990a) was recorded to resolve overlap amongst H^{N} - H^{N} NOEs in the 3D NOESY-HSQC spectrum. To distinguish between overlapping peaks, the experiment was performed in 3D mode

incorporating two indirect ^{15}N -separated dimensions. This spectrum yields cross-peaks with chemical shift coordinates $\{^{15}\text{N}(\omega_1), ^{15}\text{N}(\omega_2), ^1\text{H}(\omega_3)\}$ in contrast to $\{^1\text{H}(\omega_1), ^{15}\text{N}(\omega_2), ^1\text{H}(\omega_3)\}$ coordinates of the 3D NOESY-HSQC experiment. In the case of pairs of NOEs involving amide signals where two $^1\text{H}^{\text{N}}$ chemical shifts are degenerate but the ^{15}N chemical shifts are resolved, the ambiguity of assignment may be removed by combined analysis of the different 3D spectra. The backbone NOE assignment of HNS $_{1-64}$ is essentially complete. The pattern of secondary chemical shifts, short and medium-range interproton NOEs, and NH/solvent exchange peaks (Figure 3) was analysed to determine the secondary structure of H-NS $_{1-64}$. The structure is characterised by three α -helices, two short and one long: helix 1 (H1) spans residues 2 to 8; helix 2 (H2) spans residues 12 to 20; and helix 3 (H3) spans residues 22 to 53.

In addition we investigated the residue-specific dynamic properties of the polypeptide backbone of ^{15}N -labelled H-NS $_{1-64}$ using ^{15}N nuclear relaxation measurements, including longitudinal (T_1) and transverse (T_2) ^{15}N relaxation time constants, and the magnitude of $\{^1\text{H}\}^{15}\text{N}$ heteronuclear NOEs (see

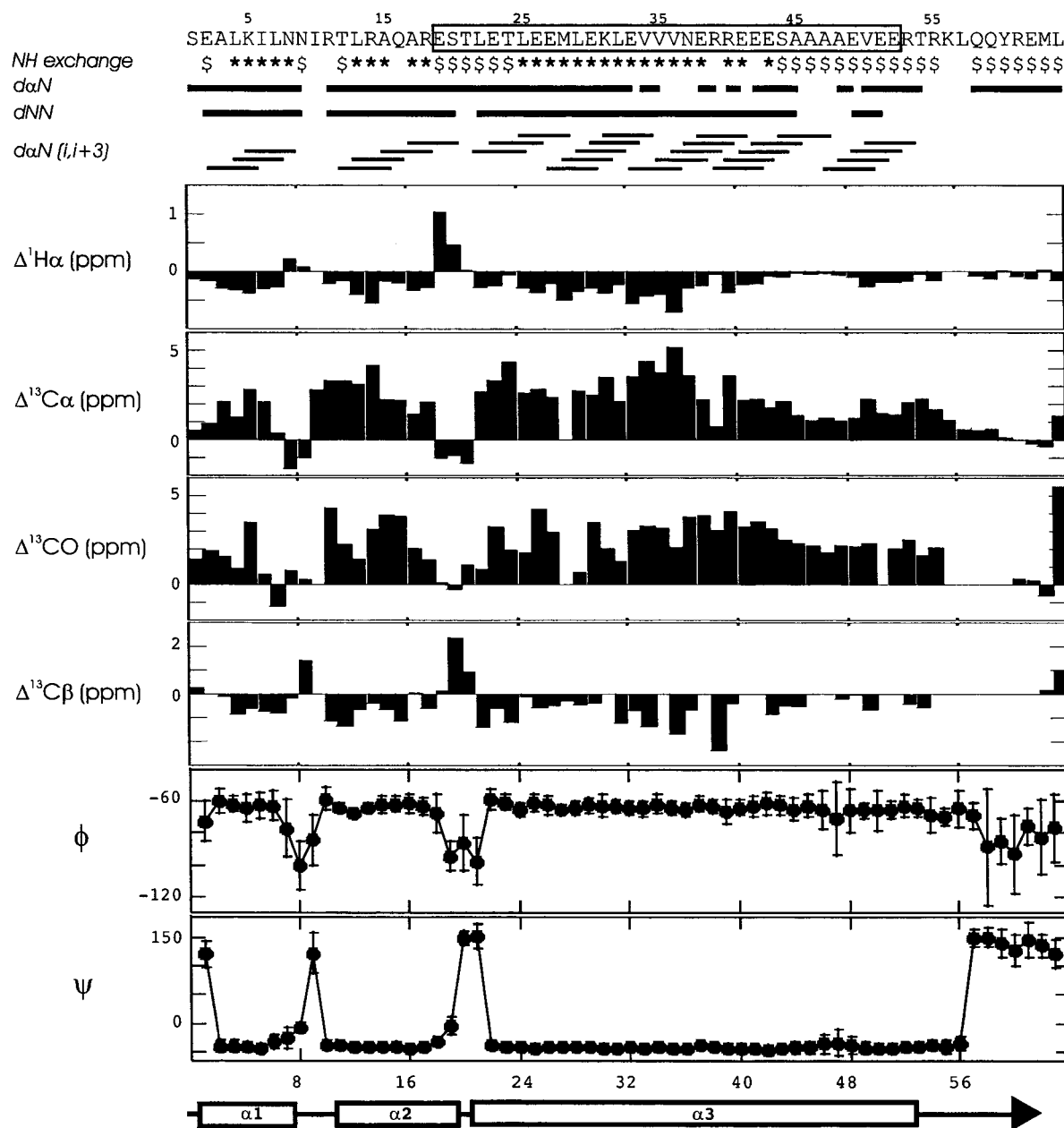


Figure 2. A summary of the NMR parameter used to analyse the secondary structure of H-NS₁₋₆₄. The first four N-terminal residues (GSHM) of the expressed polypeptide, extraneous to wild-type H-NS, are not included in the primary sequence. The residues predicted to be in a coiled-coil structure (with a probability higher than 90%) using the COILS program (Lupas *et al.*, 1996) are boxed. NH/solvent exchange rates were qualitatively monitored from the presence or absence of amide proton/solvent exchange peaks in the 3D ¹⁵N-separated NOESY-HSQC spectrum. The \$ sign indicates the presence of a solvent exchange cross-peak; the * sign indicates the absence of a cross-peak to water and a blank space indicates uncertainty arising from α proton signals close to the water resonance. Blank spaces in the $d_{\alpha N}$, d_{NN} and $d_{\alpha N}(i,i+3)$ NOE summary sections represent either an uncertain assignment due to overlapping peaks or the absence of cross-peaks corresponding to these connectivities. The chemical shift values of ¹³C α , ¹³CO and ¹³C β derived from the NMR spectra of the perdeuterated sample of H-NS₁₋₆₄ used to calculate the secondary chemical shift values and to run the computer program TALOS, were corrected according to the values reported (Gardner *et al.*, 1997). TALOS was also run on the incomplete set of chemical shifts obtained from spectra recorded at 36 °C on a protonated sample of H-NS₁₋₆₄. The two sets of TALOS results were extremely similar and qualitatively identical. At the bottom the schematic representation of the secondary structure of H-NS₁₋₆₄ (helices H1, H2 and H3) summarises the prediction that arises out of the inspection of the pattern of experimental NMR data.

Figure 3). Measurements were recorded with three different dilutions of the sample. The ¹⁵N relaxation parameters were analysed in the mode of

standard model-free treatment (Lipari & Szabo, 1982; Kristensen *et al.*, 2000), initially with the assumption of isotropic rotational diffusion, to

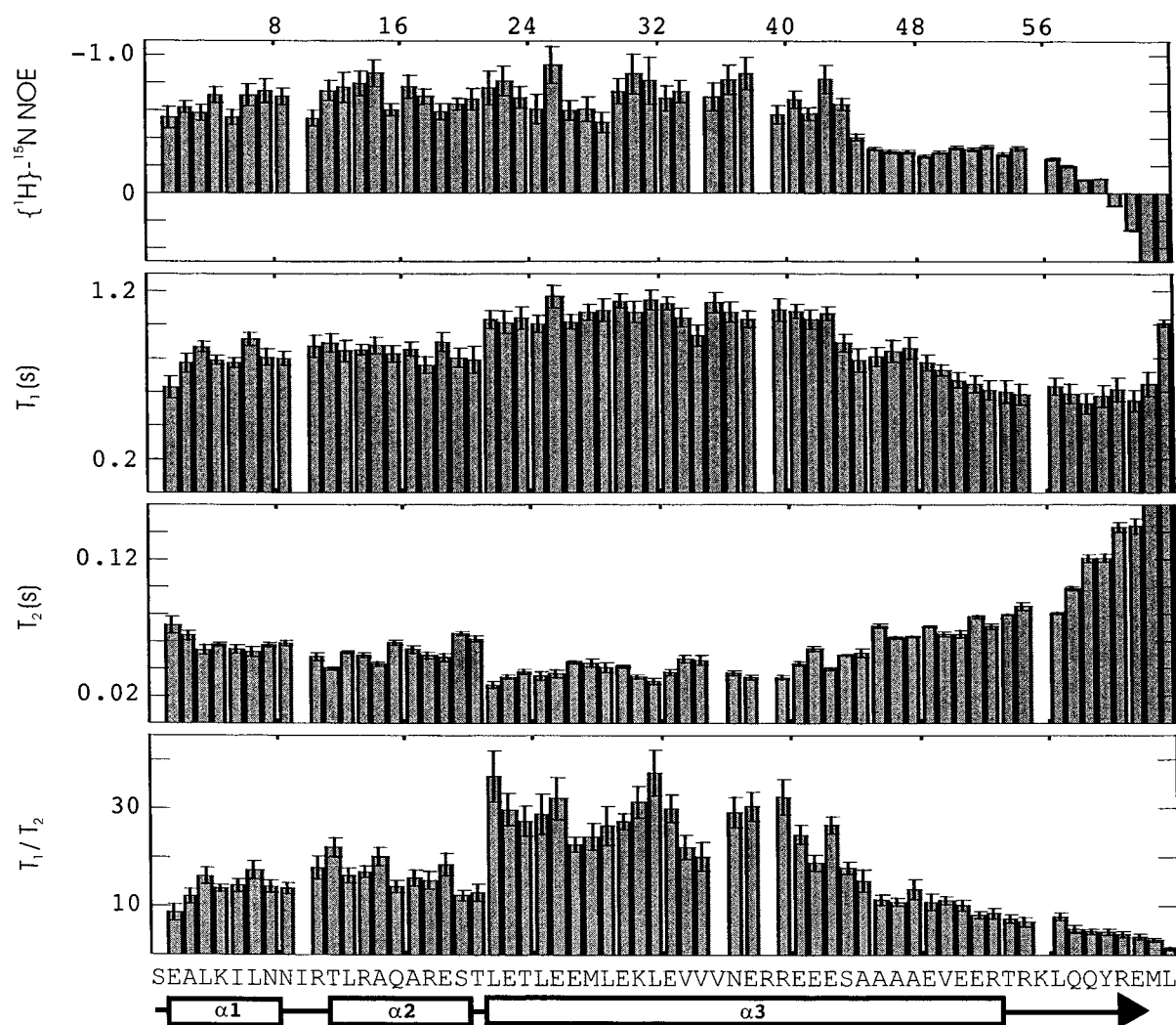


Figure 3. A summary of the ^{15}N nuclear relaxation parameters determined for ^{15}N -labelled HNS_{1-64} . Steady-state heteronuclear $\{^1\text{H}\}^{15}\text{N}$ NOE values, along with ^{15}N T_1 and ^{15}N T_2 relaxation data and T_1/T_2 ratios plotted against the primary sequence and secondary structure of H-NS_{1-64} .

extract the apparent isotropic molecular rotational correlation times. This analysis yielded values of the apparent rotational correlation time for the H-NS_{1-64} of $\tau_c = 10.62(\pm 0.40)$ ns, $\tau_c = 11.69(\pm 0.37)$ ns, and $\tau_c = 12.44(\pm 0.37)$ ns corresponding to protomer (homotrimer) concentrations of 0.25 (0.083) mM, 0.5 (0.17) mM, and 1.5 (0.5) mM, respectively. Over the range of polypeptide concentration examined there was no systematic variation of cross-peak chemical shifts, and no indication of chemical exchange phenomena giving rise to isolated outlying values of the transverse relaxation rates. The overall pattern of nuclear relaxation rates was preserved across the polypeptide sequence (data not shown), suggesting that the concentration-dependent variation in relaxation parameters can be attributed to weak, non-specific self-association of H-NS_{1-64} homotrimers. As this affects all residues to the same extent, the T_1/T_2 ratios are scaled accordingly. Thus, the profile of

their distribution, important in the anisotropy analysis, is unaffected.

Examination of the profile of the H-NS_{1-64} ^{15}N nuclear relaxation parameters (Figure 3) reveals a starkly non-uniform distribution of values. Simple inspection of the profiles in Figure 3 reveals apparent steps in the profile of T_1 and T_2 values and T_1/T_2 ratios. In combination with the experimentally predicted secondary structure of the polypeptide (Figure 2) it is clear that the data for helix 3 (H3) are divided into two distinct regions. The first region comprises residues L22 ~ A45 which possesses characteristics of a rigid, canonical α -helix (S2, secondary shifts). However for the section of the polypeptide running from A46 to the C-terminal end of H3 at residue R53 some form of intermediate state is apparent. For this latter region the secondary chemical shifts are still predictive of helical structure, but with somewhat diminished magnitudes compared to the corresponding values

for residues L22-A45. In addition, protection of the amide groups from solvent exchange is detected only for residues L22-A45; residues to the C-terminal side of this section all yield NH/H₂O solvent exchange cross-peaks. Further evidence of the variation of structural characteristics within H3 is revealed by the pattern of $\{^1\text{H}\}^{15}\text{N}$ heteronuclear NOEs which exhibit values around 0.8 throughout the first part of the helix but drop to ~ 0.5 from residue A45 onwards, decreasing to values of below zero for the extreme flexible C terminus (Figure 3). Unresolved overlap of H^N signals and poor resolution of the H^α region in the 3D ^{15}N NOESY-HSQC spectrum prevented the unambiguous assignment of intra-chain H^N-H^N and medium-range NOE with absolute certainty for T54, R55 and K56 and therefore precluded the definition of the conformation adopted by these residues. The region from residue K56 to the C terminus appears to be strongly disordered. Comparison of peak intensity ratios between 2D ^{15}N -HSQC spectra recorded on fresh samples and samples that had suffered some adventitious proteolysis (as a function of age) showed that H-NS₁₋₆₄ undergoes degradation of the chain at sites downstream of residue T54. Since stable α -helices are not easily accessible to protease action, this observation is consistent with the lack of regular secondary structure at the C terminus of the polypeptide.

The computer program TALOS (Cornilescu *et al.*, 1999) was used to obtain predicted upper and lower bounds on the Φ and Ψ backbone torsion angles for H-NS₁₋₆₄. The TALOS program used the experimental input secondary chemical shifts to search a "protein-of-known-structure chemical shift database" for instances of strings of residues with chemical shift similarity and residue type homology. The values of Φ and Ψ torsion angles derived with TALOS (Figure 2) from the chemical shifts of H-NS₁₋₆₄ are fairly consistent, for most residues, with the secondary structure predicted from manual inspection of NMR parameters reported in Figure 2. Discrepancies arise only for the dihedral angle prediction for single residues at the very ends of the three helical regions.

Model of the global topological fold of H-NS₁₋₆₄

The unusual pattern of ^{15}N relaxation parameters within the apparent core regions of the H-NS₁₋₆₄ polypeptide chain have prompted us to examine whether these data can be analysed in an internally consistent manner with a model of the structure that allows for rotational diffusion anisotropy. It is well known that the relationship between distribution of heteronuclear ^{15}N T_2 and T_1 relaxation times and the magnitude of anisotropic rotational diffusion can provide information on the spatial arrangement of the N-H bond vectors relative to a single molecular reference frame (Tjandra *et al.*, 1995, 1997). In the absence of any structural information, the analysis of the experimental distribution of the T_1/T_2 ratios can yield

an estimate of the degree of symmetry and the magnitude of the components D_{xx} , D_{yy} and D_{zz} of the molecular rotational diffusion tensor in the principal axis system (Clore *et al.*, 1998). In Figure 4 we demonstrate, by simple mathematical modelling, that the distribution of ^{15}N T_1/T_2 ratios yields patterns that are strongly characteristic of the type and degree of rotational diffusion anisotropy present. As a result we can relate the overall shape of the polypeptide to the relaxation data. Figure 4 also reports the histogram representing the distribution of the experimental ^{15}N T_1/T_2 ratios obtained for H-NS₁₋₆₄. The one-sided shape of the distribution corresponds to what would be predicted for an axially symmetric rotational diffusion tensor where $D_{zz} \neq D_{xx} = D_{yy}$. We note that for a parallel symmetric oligomer with number of polypeptide chains ≥ 3 the rotational diffusion tensor will be, by definition, axially symmetric. It should be noted that whilst the experimental data shown in Figure 4 correspond to a H-NS₁₋₆₄ protomer concentration of 1.5 mM (homotrimer concentration 0.5 mM), essentially identical distributions where

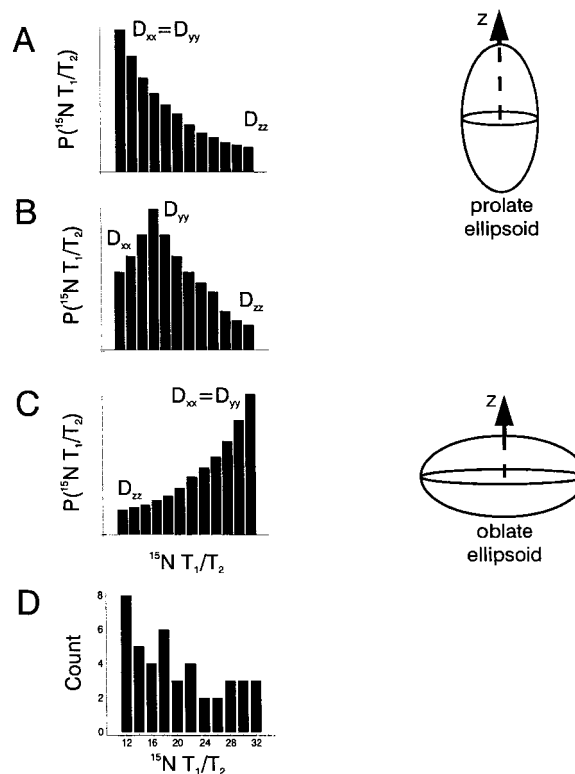


Figure 4. (a)-(c) Simulations of the distribution of ^{15}N T_1/T_2 values that would be obtained for molecules with (a) axially symmetric prolate (shown diagrammatically), (b) non-axially symmetric, and (c) oblate (shown diagrammatically) rotational diffusion tensors. (d) Experimental distribution of ^{15}N T_1/T_2 values for H-NS₁₋₆₄ measured at 600 MHz. The highest and lowest values in the histogram corresponding to $(T_1/T_2)_{\text{max}}$ and $(T_1/T_2)_{\text{min}}$ used to obtain the components of the axially symmetric diffusion tensor are 32.1 and 11.0, respectively.

obtained at the two lower concentrations tested (*vide infra*, data not shown).

In the case of an axially symmetric diffusion tensor and in the absence of large amplitude internal motion ($S > 0.9$) the ^{15}N T_1/T_2 ratio for a single NH group depends only on the angle θ and the diffusion tensor components D_{\parallel} and D_{\perp} (see Experimental Procedures). Assuming good sampling of NH bond vector directions in the experimental distribution the highest value of the T_1/T_2 ratio, $(T_1/T_2)_{\text{max}}$, corresponds to a bond vector lying along the z-axis of the diffusion tensor ($\theta \approx 0^\circ$) whilst the lowest value of the T_1/T_2 ratio, $(T_1/T_2)_{\text{min}}$, corresponds to a vector in the x-y plane. A best-fitting procedure based on the equations (1)-(3) (see Experimental Procedures) and the extracted values of $(T_1/T_2)_{\text{min}}$ and $(T_1/T_2)_{\text{max}}$ allows the determination of the D_{\parallel} and D_{\perp} components of the diffusion tensor. With knowledge of D_{\parallel} and D_{\perp} it is possible to extract, using the values of the T_1/T_2 ratio, an estimate of the angle θ for individual NH bonds. For H-NS₁₋₆₄ this procedure can be exploited to define the relative orientation of the three α -helical segments in the structure. With the assumption that the N-H bond vectors within a single helical fragment are oriented approximately parallel with the helical axis it is possible to calculate an average value for the angle formed by each helix of HNS₁₋₆₄ with the unique axis of the diffusion tensor. Values for T_1/T_2 are available for 54 backbone NH groups (Figure 3), of which (two for helix 1, six for helix 2 and 29 for helix 3) 43 yielded an experimental uncertainty smaller than ± 2 . These correspond to residues with $S > 0.9$, $\{^1\text{H}\}^{15}\text{N}$ NOE > 0.4 and exclude residues with evidence of any exchange contribution to T_2 , i.e. those residues lacking substantial internal motion. Of these, the range of T_1/T_2 values was $(T_1/T_2)_{\text{max}} = 32(\pm 2)$, $(T_1/T_2)_{\text{min}} = 11(\pm 2)$ (Figure 4). The axially symmetric molecular diffusion tensor components calculated on the basis of the experimental ensemble are $D_{\parallel} = 2.6(\pm 0.5) \times 10^7 \text{ s}^{-1}$ and $D_{\perp} = 9.3(\pm 0.3) \times 10^6 \text{ s}^{-1}$. By averaging the derived values of θ for individual NH bonds in the three helical segments of HNS₁₋₆₄ we obtained estimates of the resulting angles that each helix forms with the z-axis of the axially symmetric diffusion tensor: H3, $23(\pm 14)^\circ$; H2, $47(\pm 12)^\circ$; and H1, $60(\pm 17)^\circ$. The variation of amide bond orientations, and consequently the variation of ^{15}N T_1/T_2 ratios, within each helical segment lead to a rather high uncertainty on the predicted angles. However it is clear that the experimental ^{15}N T_1/T_2 values indicate that the helix direction vectors are significantly divergent.

Additionally, we analysed the relaxation data for H-NS₁₋₆₄ in a variety of alternative models, including explicit allowance for a rhombic contribution (i.e. $D_{xx} \neq D_{yy}$) to the rotational diffusion tensor, which would provide scope for symmetric parallel (C_2 symmetry) or antiparallel homodimer (C_i symmetry) and "dimer of dimers" antiparallel homotetramer (C_2 symmetry) configurations of the

polypeptide. These calculations uniformly provided results where the derived rhombic component was small (D_{xx}/D_{yy} in the range 0.92 - 1.0) and yielded only small variations on the derived helix direction angles (data not shown). This is entirely to be expected given the one-sidedness of the distribution of ^{15}N T_1/T_2 ratios shown in Figure 3. Along with the experimental observations of the trimeric nature of H-NS₁₋₆₄ (Smyth *et al.*, 2000) and the magnetic equivalence of all protons in the homo-oligomer, these analyses strongly support the conclusion that the structure of the polypeptide is consistent with a parallel-homotramer (C_3 -symmetry axis) with an axially symmetric rotational diffusion tensor.

Due to the angular dependence and the degeneracy of the second-rank axially symmetric diffusion tensor, each calculated helix direction angle corresponds to a conical surface about the axis of the diffusion tensor upon which the position of the helix is constrained (Figure 5). It is reasonable to suppose that the axial symmetry of the diffusion tensor reflects the overall symmetry of the H-NS₁₋₆₄ homotrimer structure. The axis of symmetry (i.e. the z-axis) of the diffusion tensor has necessarily to be colinear with the C_3 symmetry axis of the homotrimer. Helix 3 (residues 22-53) forms the lowest angle with the unique axis of the

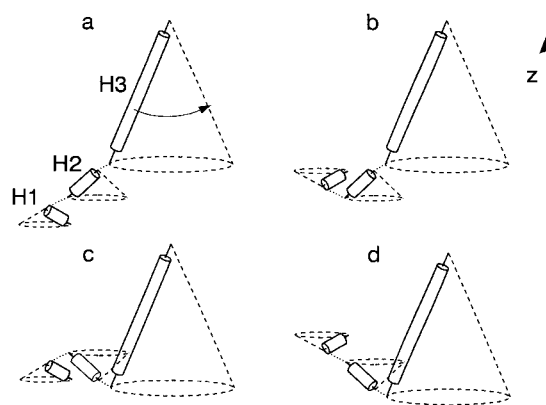


Figure 5. Overview of the models for the helix direction angles in the structure of the H-NS₁₋₆₄ protomer consistent with the anisotropic diffusion measurements. H1, H2, H3 represent the helical segments formed by residues 2-8, 12-20 and 22-53, respectively. The broken lines describe conical surfaces where the position of the helices is constrained on the basis of the ^{15}N relaxation data analysis. The angles that the helices form with the unique axis of the tensor are 23° , 47° and 60° for H3, H2, and H1, respectively. The z-axis is coincident with the C_3 symmetry axis for the parallel homotrimer in which helix H3 forms the core of the coiled-coil structure. Within the four arrangements, arising from the degeneracy of the helix directions consistent with the axially symmetric diffusion tensor, model d most resembles a previously reported structural arrangement in which short helical segments fold back to interact with the coiled-coil core of the structure (O'Hara *et al.*, 1999).

tensor, and provides high values of T_1/T_2 ratios which fall towards the right of the distribution in Figure 4. As a consequence H3 is close to the z-axis of a prolate ellipsoid structure, consistent with this region of HNS₁₋₆₄ adopting the inter-chain coiled-coil interaction surface predicted on the basis of the Leu heptad repeat (Smyth *et al.*, 2000).

The possibility of adopting different N → C or C → N orientations of each helix on its direction cone leads to a total of four different potential arrangements for a single chain within the trimeric H-NS₁₋₆₄ three-dimensional structure, as illustrated in Figure 5. At present there is no definitive evidence to support a particular choice of one arrangement for the structure over another. However, model d in Figure 5 represents a more compact structure that resembles a previously published structural motif in which the stability of a central coiled-coil fold appears to be buttressed by intramolecular interaction with short terminal α -helices (O'Hara *et al.*, 1999).

Conclusions

Here we report the first characterisation of the secondary structure of the oligomerisation domain of H-NS (residues 1-64). This study represents a significant advance in the structural and functional dissection of the H-NS protein, providing structural information on the conformation of the polypeptide within the context of the homotrimer. This self-associated state provides the basic building block for the structurally intractable, macromolecular, heterodisperse, full-length H-NS protein scaffold required for DNA packaging in bacteria. Extensive mutational studies on H-NS have described only four point mutations within the 64 N-terminal residues of H-NS that affect the protein function. Mutations at position R11, R14 and R53 affect expression of the *proV* and *bgl* operons (Ueguchi *et al.*, 1996) and a mutation of L29 affects oligomerisation and the role of H-NS as a transcription repressor (Ueguchi *et al.*, 1997). It is interesting to note that the arginine side-chain H^c frequencies of residues R11 and R14 are dramatically shifted to low field, resonating at 9.1 and 8.3 ppm, respectively (Figure 1). Such low field shifts are usually due to hydrogen bond formation. These effects probably represent intra-chain or inter-chain interactions important for the stability of the HNS₁₋₆₄ structure. This provides a rationalisation for why it is not feasible to mutate these arginine residues without disrupting the function of H-NS. Furthermore, L29 is part of the longest helix of H-NS₁₋₆₄ and is predicted in our model to be one of the residues of the hydrophobic interface of the coiled-coil forming part of the characteristic heptad repeat sequence. Thus, our structural data are able to provide insight into the mechanism by which reported mutations result in altered function from disruption of H-NS₁₋₆₄ trimer formation.

The combined analysis of experimental NMR chemical shift, NOE, NH/solvent exchange and ¹⁵N nuclear relaxation data unambiguously identify the C-terminal region (from A45 to R53) as more flexible than the rest of H3. The timescale for this flexibility is not well defined, but likely to be on the picosecond-nanosecond timescale as reflected in ¹⁵N relaxation data. The lack of dynamic stability in this region of H3 in the trimeric state raises the possibility that this region of the H-NS is involved in formation of higher oligomeric states in the full-length protein, i.e. this segment might provide a nucleation site of higher-order assembly.

One interesting feature of the structural data reported here is that H-NS₁₋₆₄ consists of three distinct α -helical segments. The first two helices (H1 and H2) are each comprised of only approximately two full turns (seven and nine residues, respectively). The third helix, H3, which spans residues 22-53, is predicted to form the core of the coiled-coil structure. Similar helical arrangements have been observed for other protein structures that contain coiled-coil elements (e.g. O'Hara *et al.*, 1999). In these structures the short helices are found in a conformation where the most N-terminal residues form intramolecular interactions with the long helix forming the central core of the coiled-coil. This helical arrangement is broadly consistent with the models in Figure 5. This motif could represent a common conformation which acts to stabilise coiled-coils.

The structural data presented here, combined with our investigation on the oligomerisation of H-NS (Smyth *et al.*, 2000), enable us to speculate that the packaging of bacterial DNA involves the interaction of the homotrimeric subunits, which are able to stack to form a multimolecular scaffold. Based on the limitation in the number of monomers that can be associated *via* a coiled-coil structure with the symmetry properties described for H-NS₁₋₆₄ it is likely that the trimers interact *via* their N and/or C termini. The C-terminal domain is able to independently interact with DNA, since the flexible linker between it and the N-terminal oligomerisation domain provides significant freedom of motion.

Experimental Procedures

Sample preparation

Escherichia coli BL21 (λ DE3) cells were transformed with a pET_{14b} plasmid encoding N-terminally His₆-tagged H-NS₁₋₆₄ as described previously (Smyth *et al.*, 2000). When uniform ¹⁵N and ¹⁵N/¹³C labelling was carried out, the bacteria were grown in M9 minimal medium using ¹⁵NH₄SO₄/¹²C₆-glucose and ¹⁵NH₄SO₄/¹³C₆-glucose as the sole nitrogen and carbon sources, respectively: 500 ml flasks containing 150 ml of LB medium (Luria Bertani) and carbenicillin (100 μ g/ml) were inoculated with cells from a freshly transformed colony. The pellet from 10 ml of the overnight cultures was used to inoculate 2 l flasks containing 500 ml of M9 minimal

medium and carbenicillin and grown in a shaking incubator at 200 rpm and 37 °C until an A_{600} of 0.5 was reached. The T7 promoter was then induced by addition of isopropyl- β -D-thiogalactopyranoside (IPTG; Melford Laboratories Ltd.) to a final concentration of 0.5 mM and incubated at 200 rpm and 37 °C for four hours. The cells were centrifuged at 5000 rpm in a SORVALL GS3 rotor and the resulting cell pellet was stored at -70 °C.

Perdeuteration (>95% at C α positions) and uniform $^{15}\text{N}/^{13}\text{C}$ isotope labelling of the polypeptide was achieved by growing the bacteria in M9 minimal medium with $^2\text{H}_2\text{O}$ instead of H_2O and using $^{15}\text{NH}_4\text{SO}_4/^{13}\text{C}_6$ -glucose as the sole nitrogen and carbon sources: 10 ml vials containing 5 ml of LB medium (Luria Bertani) and carbenicillin (100 $\mu\text{g}/\text{ml}$) were inoculated with cells from a freshly transformed colony. The pellets from these 10 ml LB cultures, left to grow for four hours, were used to inoculate 50 ml of M9 medium in H_2O , with 100 $\mu\text{g}/\text{ml}$ carbenicillin, in a 500 ml flask and grown in a shaking incubator at 200 rpm and 37 °C until an A_{600} of 0.4 was reached. The pellet from this 50 ml culture was used to inoculate 200 ml of M9 minimal medium in $^2\text{H}_2\text{O}$ with the same amount of carbenicillin in a 500 ml flask and grown in a shaking incubator at 200 rpm and 37 °C until an A_{600} of 0.5 was reached. The pellet from this 200 ml culture was used to inoculate 2×500 ml of M9 minimal medium in $^2\text{H}_2\text{O}$ and carbenicillin in 2 l flasks and grown in a shaking incubator at 200 rpm and 37 °C until an A_{600} of 0.5 was reached. The T7 promoter was then induced by addition of IPTG to a final concentration of 0.5 mM and incubated at 200 rpm and 37 °C for five hours. The cells were centrifuged at 5000 rpm in a Sorvall GS3 rotor and the resulting cell pellet was stored at -70 °C.

The purification of H-NS $_{1-64}$ was performed as reported (Smyth *et al.*, 2000). Recombinant H-NS $_{1-64}$ contains four additional N-terminal residues GSHM (designated here as -4, -3, -2 and -1), extraneous of wild-type H-NS, and the first 64 residues of H-NS (designated here 1 to 64). Since *in vivo* H-NS from *S. typhimurium* undergoes post-translational modifications which result in the cleavage of the methionine residue at the N terminus, here residue number 1 (serine) is defined as the residue immediately following cleaved methionine (-1). The size and homogeneity (>95% in all cases) of the purified polypeptide was confirmed by denaturing SDS/polyacrylamide gel electrophoresis and staining with Coomassie brilliant blue R-250. The mass of the polypeptide was confirmed using mass spectrometry (M_r of H-NS $_{1-64}$ 7958 g mol $^{-1}$).

NMR spectroscopy

NMR spectra were acquired on a Varian UNITYplus 500 MHz, a Varian UNITYplus 600 MHz and a Bruker AVANCE 800 MHz spectrometer at temperatures ranging between 25 °C and 36 °C. The experiments recorded on ^{15}N -labelled polypeptide were 2D ^{15}N HSQC (Bodenhausen & Ruben, 1980); ^1H NOESY (Kumar *et al.*, 1980); ^1H TOCSY (Braunschweiler & Ernst, 1983); ^{15}N NOESY-HSQC (Ikura *et al.*, 1990); 3D version of the 4D $^{15}\text{N},^{15}\text{N}$ HSQC-NOESY-HSQC (Kay *et al.*, 1990a); ^{15}N -separated TOCSY-HSQC (Gronenborn *et al.*, 1989); HNHA (Kay & Bax, 1990); $\{^1\text{H}\}^{15}\text{N}$ steady-state NOE; ^{15}N T_1 and T_2 relaxation experiments (Kay *et al.*, 1989, 1992a). The experiments recorded on $^{15}\text{N}/^{13}\text{C}$ -labelled samples were ^{13}C -separated NOESY-HSQC (Zuiderweg *et al.*, 1990); ^{13}C HCCH-TOCSY (Bax *et al.*, 1990); HNCA,

HNCO, HN(CO)CA, HN(CA)CO (Kay *et al.*, 1990b); HNCACB (Wittekind & Mueller, 1993); HN(CO)CACB (Grzesiek & Bax, 1992); HCCH ^{13}C - ^{13}C NOE (Fischer *et al.*, 1996). The 3D experiments recorded on triple $^2\text{H}/^{15}\text{N}/^{13}\text{C}$ -labelled samples were HNCA, HN(CO)CA, HN(COCA)CB, HN(CA)CB, HN(CA)CO (Yamazaki *et al.*, 1994) and HNCO. The ^{15}N nuclear relaxation experiments were recorded and analysed essentially as described by Kristensen *et al.* (2000). Unless indicated otherwise, all H-NS $_{1-64}$ samples were dissolved in 90% $\text{H}_2\text{O}/10\%$ $^2\text{H}_2\text{O}$, containing 300 mM NaCl, 20 mM potassium phosphate, 1 mM EDTA, at pH 7.0. The monomer concentration of the polypeptide ranged between 1 and 2 mM (measured using UV absorption at 280 nm with $\epsilon_{280} = 1280 \text{ M}^{-1} \text{ cm}^{-1}$).

A mixing time of 80 ms was used in all NOE experiments, except for the HCCH ^{13}C - ^{13}C NOESY spectrum where a 1.2 seconds mixing time was used. The 2D ^1H TOCSY and the 3D ^{15}N -separated TOCSY-HSQC employed mixing times of 50 and 32 ms, respectively, using the TOWNY sequence (Kadkhodaei *et al.*, 1993).

With the exception of the ^{13}C - ^{13}C NOE experiment all heteronuclear NMR spectra were recorded with gradient sensitivity enhancement in the first indirect heteronuclear dimension of the 2D and 3D experiment (Kay *et al.*, 1992b). Indirect dimensions were processed after appropriate rearrangements of FIDs according to the States-TPII procedure (States *et al.*, 1982). Chemical shift calibrations for all nuclei were performed relative to the proton resonance of DSS as suggested previously (Wishart *et al.*, 1995). Spectra were processed with NMRPIPE (Delaglio *et al.*, 1995) and analysed with AZARA 2.0 (Boucher, 1996) and ANSIG (Kraulis, 1989).

Data analysis for the model of the global topological fold of H-NS $_{1-64}$

The parallel and perpendicular components of an axially symmetric diffusion tensor are defined as $D_{\parallel} = D_{zz}$ and $D_{\perp} = (D_{xx} + D_{yy})/2$, respectively. The spectral density function for a prolate ellipsoid is given by (Lipari & Szabo, 1982):

$$J(\omega) = S^2 \sum_{k=1,2,3} A_k \left[\frac{\tau_k}{1 + \omega^2 \tau_k^2} \right] \quad (1)$$

where ω is the angular frequency and S the generalised order parameter for rapid internal motion. τ_1 , τ_2 and τ_3 are time constants and are defined as follows: $\tau_1 = (6D_{\perp})^{-1}$, $\tau_2 = (D_{\parallel} + 5D_{\perp})^{-1}$ and $\tau_3 = (4D_{\parallel} + 2D_{\perp})^{-1}$; the terms A_1 , A_2 and A_3 are given by $A_1 = (1.5\cos^2\theta - 0.5)^2$, $A_2 = 3\sin^2\theta\cos^2\theta$ and $A_3 = 0.75\sin^4\theta$ where θ is the angle between the N-H bond vector and the z-axis of the diffusion tensor. The ^{15}N T_1 and T_2 relaxation times can be expressed in terms of spectral density function $J(\omega)$ as (Abragham, 1961):

$$\frac{1}{T_1} = d[J(\omega_H = \omega_N) + 3J(\omega_N) + 6J(\omega_H + \omega_N)] + cJ(\omega_N) \quad (2)$$

$$\frac{1}{T_2} = \frac{d}{2} [4J(0) + J(\omega_H - \omega_N) + 3J(\omega_N) + 6J(\omega_H) + 6J(\omega_H + \omega_N)] + \frac{c}{6} [3J(\omega_N) + 4J(0)] \quad (3)$$

where the terms d and c contain constants such as the gyromagnetic ratios and the Larmor frequencies of the two nuclei, the distance between the nuclei, and the components of the axially symmetric ^{15}N chemical shift tensor (Abragam, 1961).

Acknowledgements

The authors thank Dr Kevin Gardner for the protocol to produce perdeuterated proteins and Dr Daniel Nietlisplach for assistance with recording NMR data at 800 MHz at the BBSRC National 800 MHz NMR Centre in Cambridge. Thanks also to Dr M. A. Williams for critical reading of the manuscript.

During the course of this work D.R. was supported by a European Union Training and Mobility of Researchers Fellowship and D.E. by the Biotechnology and Biological Sciences Research Council (BBSRC); M.P. is a Royal Society University Research Fellow; J.C.D.H. is grateful for the support of a Wellcome Trust Programme Grant (045490); C.F.H. is supported by the Medical Research Council; J.E.L. is a Wellcome Trust Senior Research Fellow. This work was funded by a grant to J.E.L. and P.C.D. from BBSRC. Additional funds were provided by the Wellcome Trust.

References

- Abragam, A. (1961). *The Principles of Nuclear Magnetism*, Clarendon Press, Oxford, England.
- Bax, A., Clore, M. & Gronenborn, A. M. (1990). ^1H - ^1H Correlation *via* isotropic mixing of ^{13}C magnetization, a new three-dimensional approach for assigning ^1H and ^{13}C spectra of ^{13}C -enriched proteins. *J. Magn. Reson.* **87**, 425-429.
- Bertin, P., Lejeune, P., Laurent-Winter, C. & Danchin, A. (1990). Mutations in *bg1Y*, the structural gene for the DNA-binding protein H1, affect the expression of several *Escherichia coli* genes. *Biochimie*, **72**, 889-891.
- Bodenhausen, G. & Ruben, D. J. (1980). Heteronuclear 2D correlation spectra with double in-phase transfer steps. *Chem. Phys. Letters*, **69**, 185-189.
- Boucher, W. (1996). *AZARA v2.0*, Department of Biochemistry, University of Cambridge, UK.
- Braunschweiler, L. & Ernst, R. R. (1983). Coherence transfer in liquids by an average Hamiltonian. *J. Magn. Reson.* **53**, 521-524.
- Clore, G. M., Gronenborn, A., Szabo, A. & Tjandra, N. (1998). Determining the magnitude of the fully asymmetric diffusion tensor from heteronuclear relaxation data in the absence of structural information. *J. Am. Chem. Soc.* **120**, 4889-4890.
- Cornilescu, G., Delaglio, F. & Bax, A. (1999). Protein backbone angle restraints from searching a database for chemical shift and sequence homology. *J. Biomol. NMR*, **13**, 289-302.
- Delaglio, F., Grzesisek, S., Vuister, G. W., Zhu, G., Pfeifer, J. & Bax, A. (1995). NMR-Pipe. A multidimensional spectral processing system based on UNIX pipes. *J. Biomol. NMR*, **6**, 277-293.

- Drlica, K. & Rouviere-Yaniv, J. (1987). Histone-like proteins of bacteria. *Microbiol. Rev.* **51**, 301-319.
- Fischer, M. W. F., Zeng, L. & Zuiderweg, E. R. P. (1996). Use of ^{13}C - ^{13}C NOE for the assignment of NMR lines of larger labeled proteins at larger magnetic fields. *J. Am. Chem. Soc.* **118**, 12457-12458.
- Gardner, K. H., Rosen, M. K. & Kay, L. E. (1997). Global folds of highly deuterated, methyl-protonated proteins by multidimensional NMR. *Biochemistry*, **36**, 1389-1401.
- Gronenborn, A. M., Bax, A., Wingfield, P. T. & Clore, M. (1989). A powerful method of sequential proton resonance assignment in proteins using relayed ^{15}N - ^1H multiple quantum coherence spectroscopy. *FEBS Letters*, **243**, 93-98.
- Grzesiek, S. & Bax, A. (1992). Correlating backbone amide and side-chain resonances in larger proteins by multiple relayed triple resonance NMR. *J. Am. Chem. Soc.* **114**, 6291-6293.
- Higgins, C. F., Hinton, J. C. D., Hulton, C. S. J., Owen-Hughes, T., Pavitt, G. D. & Seirafi, A. (1990). Protein H1: a role for chromatin structure in the regulation of bacterial gene expression and virulence? *Mol. Microbiol.* **4**, 2007-2012.
- Ikura, M., Bax, A., Clore, M. & Gronenborn, A. M. (1990). Detection of nuclear Overhauser effects between degenerate amide proton resonances by heteronuclear three-dimensional nuclear magnetic resonance spectroscopy. *J. Am. Chem. Soc.* **112**, 9020-9021.
- Kadkhodaei, M., Hwang, T. L., Tang, J. & Shaka, A. J. (1993). A simple windowless mixing sequence to suppress cross relaxation in TOCSY experiments. *J. Magn. Reson. ser. A*, **104**, 105-107.
- Kay, L. E. & Bax, A. (1990). New methods for the measurement on NH-H^z coupling constants in ^{15}N labeled proteins. *J. Magn. Reson.* **86**, 110-114.
- Kay, L. E., Torchia, D. A. & Bax, A. (1989). Backbone dynamics of proteins as studied by ^{15}N inverse detected heteronuclear NMR spectroscopy: application to staphylococcal nuclease. *Biochemistry*, **28**, 8972-8979.
- Kay, L. E., Clore, G. M., Bax, A. & Gronenborn, A. M. (1990a). Four-dimensional heteronuclear triple-resonance NMR spectroscopy of interleukin- 1β in solution. *Science*, **4967**, 411-414.
- Kay, L. E., Ikura, M., Tschudin, R. & Bax, A. (1990b). Three-dimensional triple resonance NMR spectroscopy of isotopically enriched proteins. *J. Magn. Reson.* **89**, 496-502.
- Kay, L. E., Nicholson, L. K., Delaglio, F., Bax, A. & Torchia, D. A. (1992a). Pulse sequences for removal of the effects of cross correlation between dipolar and chemical shift anisotropy relaxation mechanism on the measurement of heteronuclear T_1 and T_2 values in proteins. *J. Magn. Reson.* **97**, 359-367.
- Kay, L. E., Keifer, P. & Saarinen, T. (1992b). Pure absorption gradient enhanced heteronuclear single quantum correlation spectroscopy with improved sensitivity. *J. Am. Chem. Soc.* **114**, 10663-10664.
- Kraulius, P. (1989). ANSIG: a program for the assignment of protein ^1H 2D NMR spectra by interactive graphics. *J. Magn. Reson.* **24**, 627-633.
- Kristensen, S. M., Siegal, G., Sankar, A. & Driscoll, P. C. (2000). Backbone dynamics of the C-terminal SH2 domain of the p85 α subunit of phosphoinositide 3-kinase. Effect of phosphotyrosine peptide binding

- and characterization of slow conformational exchange processes. *J. Mol. Biol.* **299**, 771-788.
- Kumar, A., Ernst, R. R. & Wuthrich, K. (1980). A two-dimensional nuclear Overhauser enhancement (2D NOE) experiment for the elucidation of complete proton-proton cross-relaxation networks in biological macromolecules. *Biochem. Biophys. Res. Commun.* **95**, 1-6.
- Laurent-Winter, C., Ngo, S., Danchin, A. & Bertin, P. (1997). Role of *Escherichia coli* histone-like nucleoid structuring protein in bacterial metabolism and stress response. Identification of targets by two-dimensional electrophoresis. *Eur. J. Biochem.* **244**, 767-773.
- LeMaster, D. M. & Richards, F. M. (1988). NMR sequential assignment of *Escherichia coli* thioredoxin utilizing random fractional deuteration. *Biochemistry*, **27**, 142-150.
- Lipari, G. & Szabo, A. (1982). Model-free approach to the interpretation of nuclear magnetic resonance relaxation in macromolecules: theory and range of validity. *J. Am. Chem. Soc.* **104**, 4546-4559.
- Lupas, A. (1996). Coiled-coils: new structures and new functions. *Trends Biochem. Sci.* **21**, 375-382.
- Marion, D., Ikura, M., Tschudin, R. & Bax, A. (1989). Rapid recording of 2D NMR spectra without phase cycling. Application to the study of hydrogen exchange in proteins. *J. Magn. Reson.* **85**, 393-399.
- O'Hara, B. P., Norman, R. A., Wan, P. T. C., Roe, S. M., Barrett, T. E., Drew, R. E. & Pearl, L. H. (1999). Crystal structure and induction mechanism of AmiC-AmiR: a ligand-regulated transcription anti-termination complex. *EMBO J.* **18**, 5175-5186.
- Shindo, H., Iwaki, T., Ieda, R., Kurumizaka, H., Ueguchi, C., Mizuno, T., Morikawa, S., Nakamura, H. & Kuboniwa, H. (1995). Solution structure of the DNA-binding domain of a nucleoid-associated protein, H-NS, from *Escherichia coli*. *FEBS Letters*, **360**, 125-131.
- Shindo, H., Ohnuki, A., Ginba, H., Katoh, E., Ueguchi, C., Mizuno, T. & Yamazaki, T. (1999). Identification of the DNA binding surface of H-NS protein from *Escherichia coli* by heteronuclear NMR spectroscopy. *FEBS Letters*, **455**, 63-9.
- Smyth, C. P., Lundbäck, T., Renzoni, D., Siligardi, G., Beavil, R., Layton, M., Sidebotham, J. M., Hinton, J. C., Driscoll, P. C., Higgins, C. F. & Ladbury, J. E. (2000). Oligomerisation of the chromatin-structuring protein H-NS. *Mol. Microbiol.* **36**, 962-972.
- Spassky, A., Rimsky, S., Garreau, H. & Buc, H. (1984). H1a, an *E. coli* DNA-binding protein which accumulates in stationary phase, strongly compacts DNA *in vitro*. *Nucl. Acids Res.* **12**, 5321-5340.
- States, D. J., Haberkorn, R. A. & Ruben, D. J. (1982). A two dimensional nuclear Overhauser experiment with pure absorption phase in 4 quadrants. *J. Magn. Reson.* **48**, 286-292.
- Tjandra, N., Feller, S. E., Pastor, R. W. & Bax, A. (1995). Rotational diffusion anisotropy of human ubiquitin from ^{15}N NMR relaxation. *J. Am. Chem. Soc.* **117**, 12562-12566.
- Tjandra, N., Garrett, D. S., Gronenborn, A. M., Bax, A. & Clore, G. M. (1997). Defining long range order in NMR structure determination from the dependence of heteronuclear relaxation times on rotational diffusion anisotropy. *Nature Struct. Biol.* **4**, 443-449.
- Torchia, D. A., Sparks, S. W. & Bax, A. (1988). Delineation of α -helical domains in deuterium staphylococcal nuclease by 2D NOE NMR spectroscopy. *J. Am. Chem. Soc.* **110**, 2320-2321.
- Ueguchi, C., Suzuki, T., Yoshida, T., Tanaka, K. & Mizuno, T. (1996). Systematic mutational analysis revealing the functional domain organization of *Escherichia coli* nucleoid protein H-NS. *J. Mol. Biol.* **263**, 149-162.
- Ueguchi, C., Seto, C., Suzuki, T. & Mizuno, T. (1997). Clarification of the dimerization domain and its functional significance for the *Escherichia coli* nucleoid protein H-NS. *J. Mol. Biol.* **274**, 145-151.
- Ussery, D. W., Hinton, J. C. D., Jordi, B. J. A. M., Granum, P. E., Seirafi, A., Stephen, R. J., Tupper, A. E., Berridge, G., Sidebotham, J. M. & Higgins, C. F. (1994). The chromatin-associated protein H-NS. *Biochimie*, **76**, 968-980.
- Williams, R. M., Rimsky, S. & Buc, H. (1996). Probing the structure, function, and interactions of the *Escherichia coli* H-NS and StpA proteins by using dominant negative derivatives. *J. Bacteriol.* **178**, 4335-4343.
- Wishart, D. S., Bigam, C. G., Yao, J., Abildgaard, F., Dyson, H. J., Oldfield, E., Markley, J. L. & Sykes, B. D. (1995). ^1H , ^{13}C and ^{15}N chemical shift referencing in biomolecular NMR. *J. Biomol. NMR*, **6**, 135-140.
- Wittekind, M. & Mueller, L. (1993). HNCACB, a high-sensitivity 3D NMR experiment to correlate amide-proton and nitrogen resonances with the α -carbon and β -carbon resonances in proteins. *J. Magn. Reson. ser. B*, **101**, 214-217.
- Yamazaki, T., Lee, W., Arrowsmith, C. H., Muhandiram, D. R. & Kay, L. (1994). A suite of triple resonance NMR experiments for the backbone assignment of ^{15}N , ^{13}C , ^2H labelled proteins with high sensitivity. *J. Am. Chem. Soc.* **116**, 11655-11666.
- Zuiderweg, E. R. P., McIntosh, L. P., Dahlquist, F. & Fesik, S. W. (1990). Three-dimensional ^{13}C -resolved proton NOE spectroscopy of uniformly ^{13}C labeled proteins for the NMR assignment and structure determination of larger molecules. *J. Magn. Reson.* **86**, 210-215.

Edited by A. R. Fersht

(Received 31 July 2000; received in revised form 18 January 2001; accepted 18 January 2001)